Electronic Supplementary Material (ESI) for Chemical Communications.
This journal is © The Royal Society of Chemistry 2023

Electronic Supplementary Materials

Hydrophobic alloy coated Zn anode for durable electrochromic devices

.

Jianwei Hu[a,1], Yingxin Zhang[a,1], Bing Xu[a], Yujia Ouyang[a], Yu Ma[a], Huanlei Wang[a], Jingwei Chen[a,*], Haizeng Li[b,c*].

[a] School of Materials Science and Engineering, Ocean University of China, Qingdao 266100, China

E-mail: chenjingwei@ouc.edu.cn

[b]Institute of Frontier & Interdisciplinary Science, Shandong University, Qingdao 266237.China

[c]Shenzhen Research Institute of Shandong University, Shenzhen 518057, China

E-mail: haizeng@sdu.edu.cn

[1]These authors contributed equally to this work.

Experimental

Materials

Zinc sulfate heptahydrate ($ZnSO_4 \cdot 7H_2O$, ≥99.5 %), copper (II) sulfate pentahydrate ($CuSO_4 \cdot 5H_2O$, ≥99.0 %), potassium chloride (KCl, ≥99.5 %), copper foil (Cu, 99.9 %), and zinc foil (Zu, 99.9 %) were purchased from Sinopharm Chemical Reagent limited corporation. Potassium ferricyanide ($K_3[Fe(CN)_6]$, ≥99.5%), iron (III) chloride hexahydrate ($FeCl_3 \cdot H_2O$, ≥99%) were purchased from Shanghai Macklin Biochemical Co., Ltd. F-doped Tin Oxide (FTO) glasses (100*100*1.1 mm, unpolished float glass, 10 Ω/sq, transmittance 80%) were purchased from Wuhan lattice Solar Technology Co., Ltd. Zn mesh1 (wire diameter of 50 μm, hole size of 1*2 mm) and Zn mesh2 (wire diameter of 30 μm, hole size of 1*1.5 mm) were purchased from Anheng Wire Mesh Co., Ltd. All the reagents are of analytical grade and used as-received without further purification.

Electrode preparation

The CuZn alloy coating layer was introduced onto the surface of Zn foil/Zn mesh or Cu foil by electrodeposition (-1.6 V, 30 min) in a mixed electrolyte containing 0.2 M zinc sulfate hexahydrate ($ZnSO_4 \cdot 7H_2O$) and 0.02 M copper sulfate ($CuSO_4 \cdot 5H_2O$). Prussian blue (PB) was obtained on transparent conductive glass (F-doped SnO_2, FTO) by galvanostatic electrodeposition (-50 μA cm^{-2}, 300 s) in a mixed electrolyte containing 0.01 M potassium ferricyanide $K_3[Fe(CN)_6]$, 0.02 M ferric chloride hexahydrate ($FeCl_3 \cdot 6H_2O$) and 0.1 M potassium chloride (KCl). In order to ensure the transparency of electrochromic battery device, two types of Zn mesh with the same active area (S1 ~0.5676 cm^2, S2 ~0.5695 cm^2, respectively but differed line width/gap (Figure S4) were attempted as the anode.

Structural and chemical characterizations

X-ray diffraction (XRD) patterns were obtained on Rigaku D/S-4800N using 40 kV, 40 mA Cu Kα radiation. Scanning electron microscope (SEM, S-4800N) was used to study the morphology of the samples, and energy dispersive X-ray spectroscopy

was also employed to image the elemental distribution. X-ray photoelectron spectroscopy (XPS, Thermo ESCALAB 250XI) with Al Kα radiation was used to analyze the chemical structures of various samples. The contact angle was quantified with the contact angle measuring instrument (JC200ODM), with 3~5 μL of 1 M $ZnSO_4$ electrolyte. The electrochromic devices were assembled using Prussian Blue (PB) cathode, and the corresponding electrochromic properties are evaluated by an Ultraviolet-visible Spectrophotometer (Shimadzu UV-2600).

Electrochemical measurements

Linear sweep voltammetry (LSV) of bare Zn and Zn@CuZn were tested in a three-electrode configuration in 1 M Na_2SO_4. The corrosion current is fitted by selecting two more symmetrical segments in the polarization region. To be specific, cathodic tafel slope potential range is set to -1.036V to -1.024V, anodic tafel slope potential range is set to -0.936V to -0.924V. Chronoamperometry (CA) was conducted at a constant polarization potential (-1.15 V). The Zn||Zn symmetric cells were assembled using Zn foils with a diameter of 12 mm. Glass fiber separators and 1 M $ZnSO_4$ were used as separator and electrolyte, respectively. The Zn||Cu and Zn||Cu@CuZn asymmetric cells were assembled using bare Cu or Cu@CuZn working electrodes. Electrochemical impedance spectroscopy (EIS) measurements of symmetric/asymmetric cells were performed in a frequency range from 100 kHz to 0.01 Hz with an amplitude of 10 mV. CV and EIS were carried out on an electrochemical workstation (CHI760E). For three-electrode testing, Pt was used as the counter electrode, Ag/AgCl (The salt bridge is saturated KCl) was used as the reference electrode, and bare Zn or Zn@CuZn electrodes were used as the working electrode. The rate performance and cycle life were tested with a NEWARE battery tester.

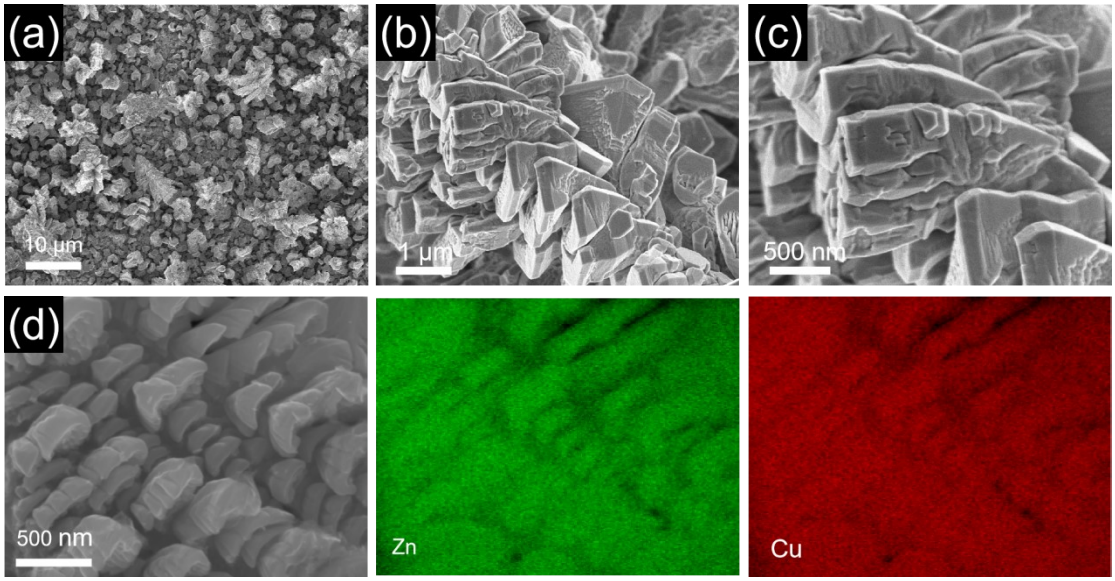

Figure S1. (a-c) SEM images of CuZn alloy coated Cu foil at different magnifications, (d) the corresponding EDX elemental mapping of the CuZn alloy coated Cu foil.

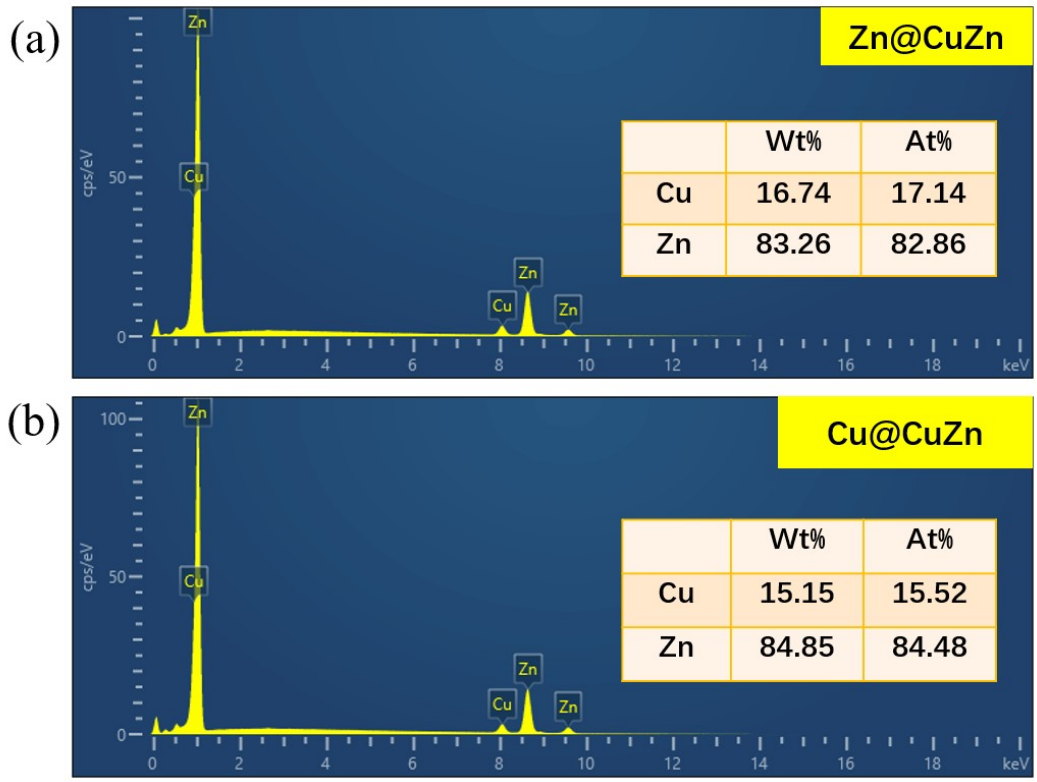

Figure S2. (a) Zn content in the CuZn layer on Zn@CuZn. (b) Zn content in the CuZn layer on Cu@CuZn.

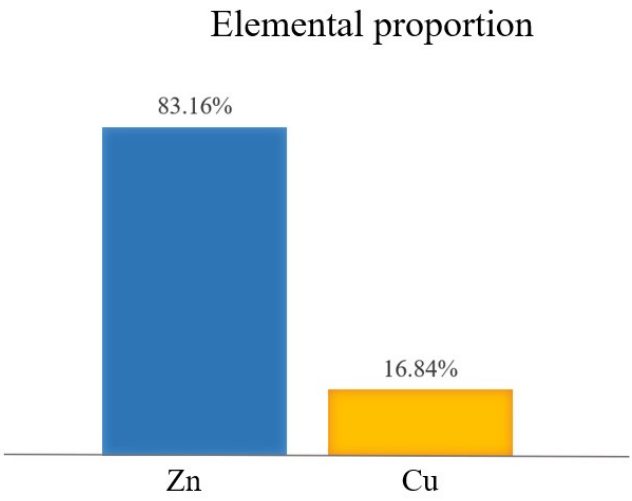

Figure S3. The ICP (inductively coupled plasma) result of $CuZn_5$.

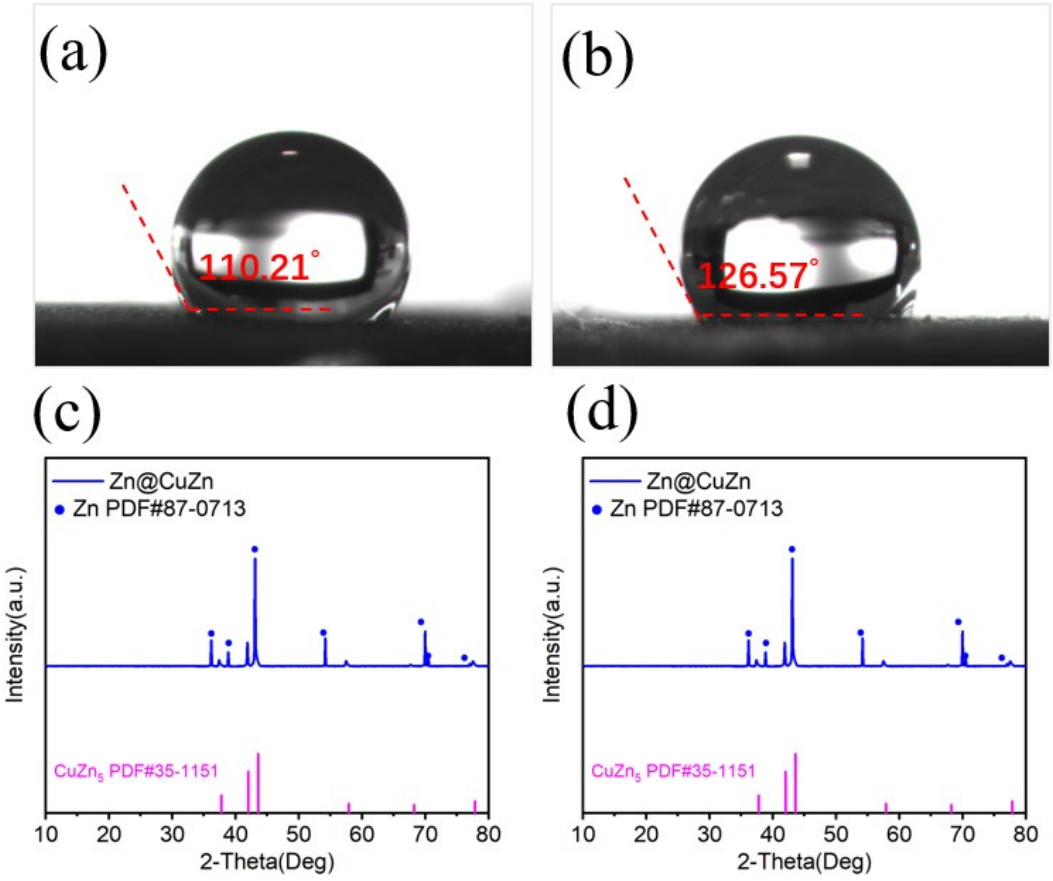

Figure S4. The contact angle of CuZn alloy deposited with (a) -1.6 V for 5 min and (b) -1.6 V for 10 min. The XRD pattern of CuZn alloy deposited with (c) -1.6 V for 5 min and (d) -1.6 V for 10 min.

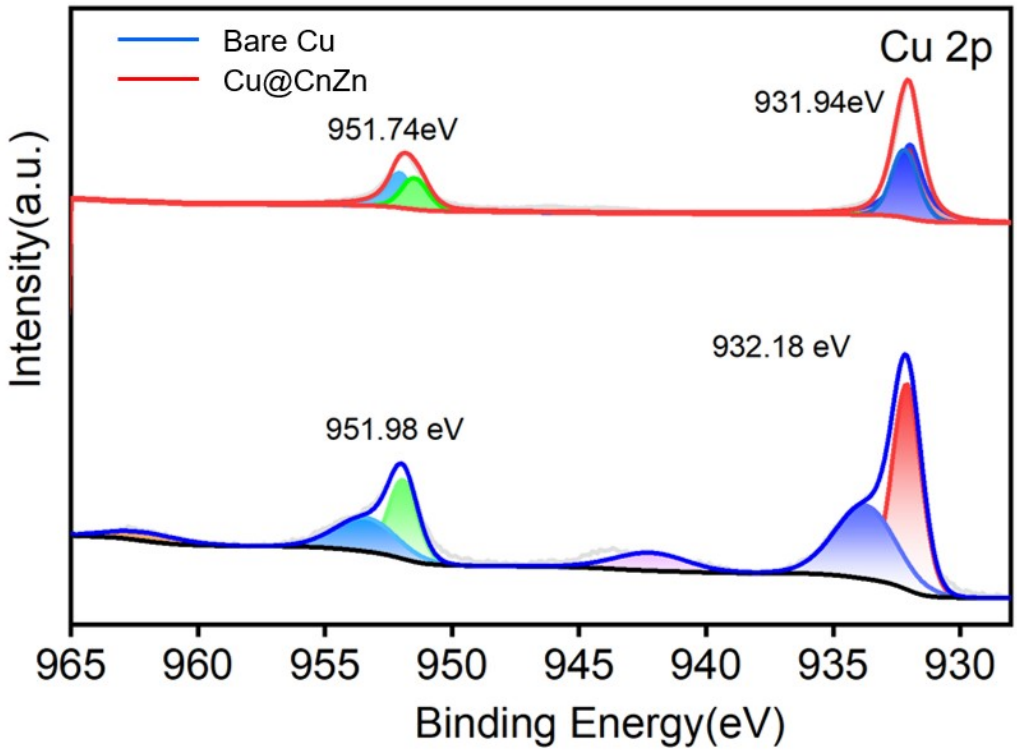

Figure S5. Cu 2p XPS spectra of bare Cu and Cu@CuZn.

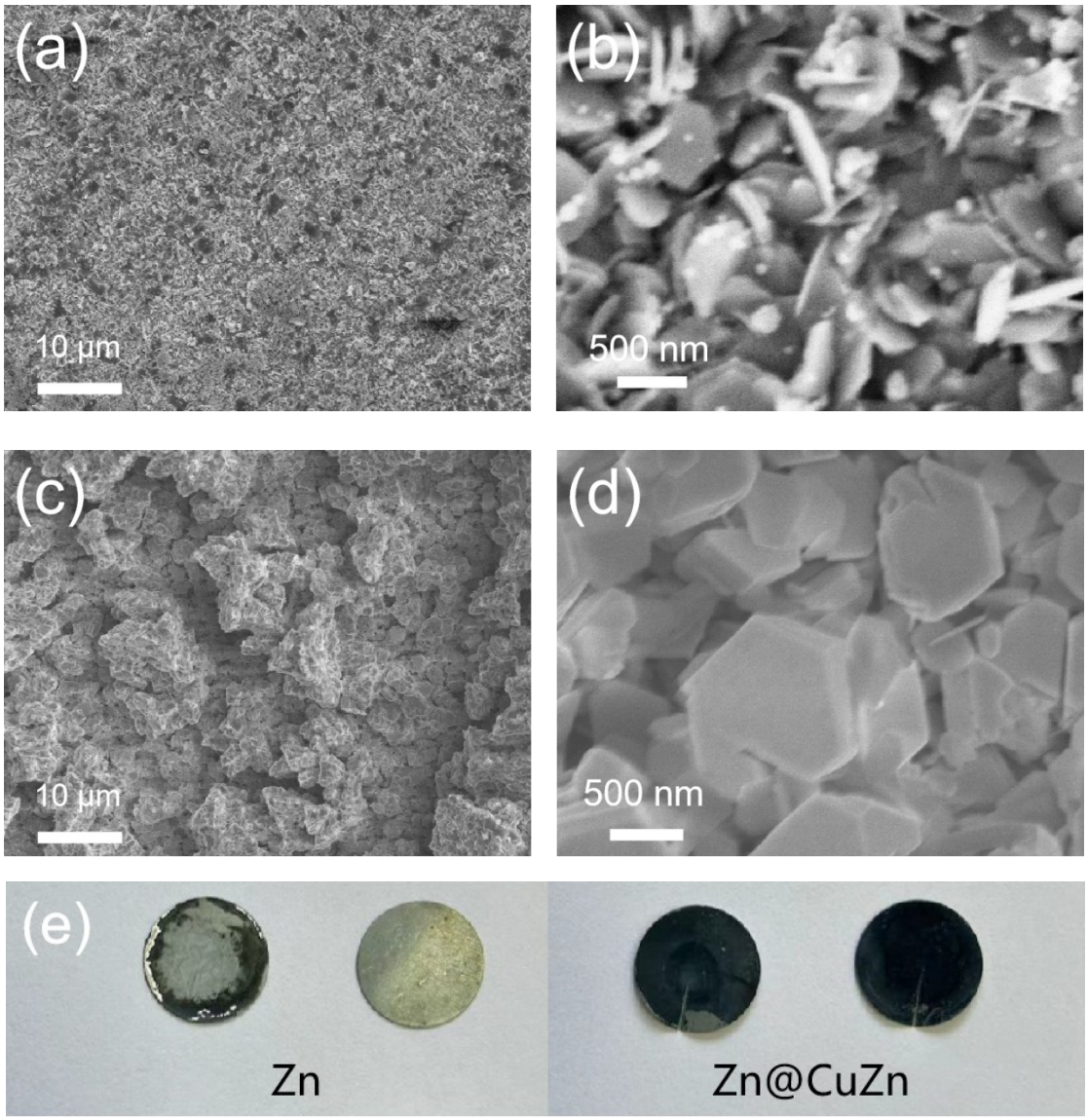

Figure S6. (a-b) SEM images of bare Zn electrode and (c-d) Zn@CuZn electrode after 1 cycle galvanostatic plating/stripping at 1 mA cm^{-2} and 1 mAh cm^{-2}. (e) Digital photographs of bare Zn electrode and Zn@CuZn electrode after 1 stripping (right) and 1 stripping/plating (left).

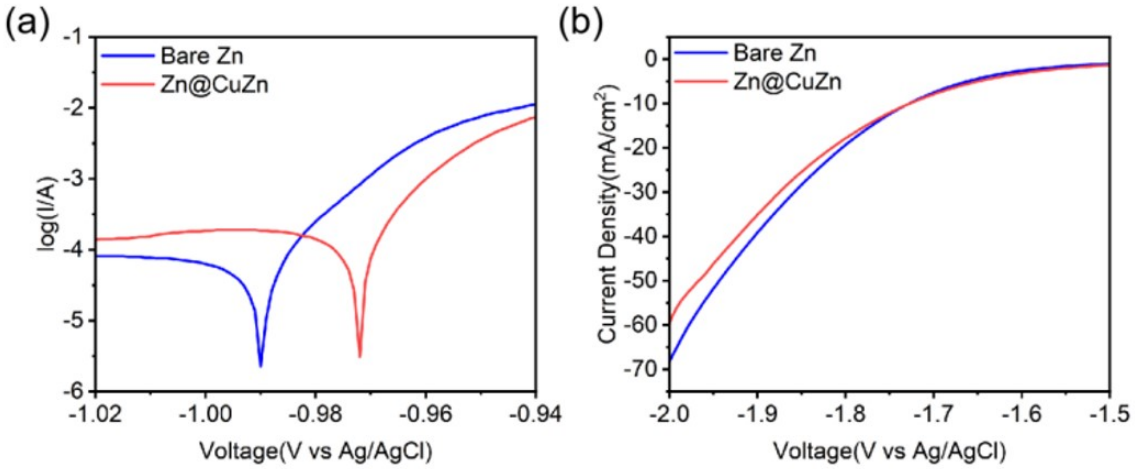

Figure S7. (a) Linear polarization curves of Zn@CuZn and bare Zn electrodes obtained with a three-electrode system. (b) LSV curves of bare Zn and Zn@CuZn for HER.

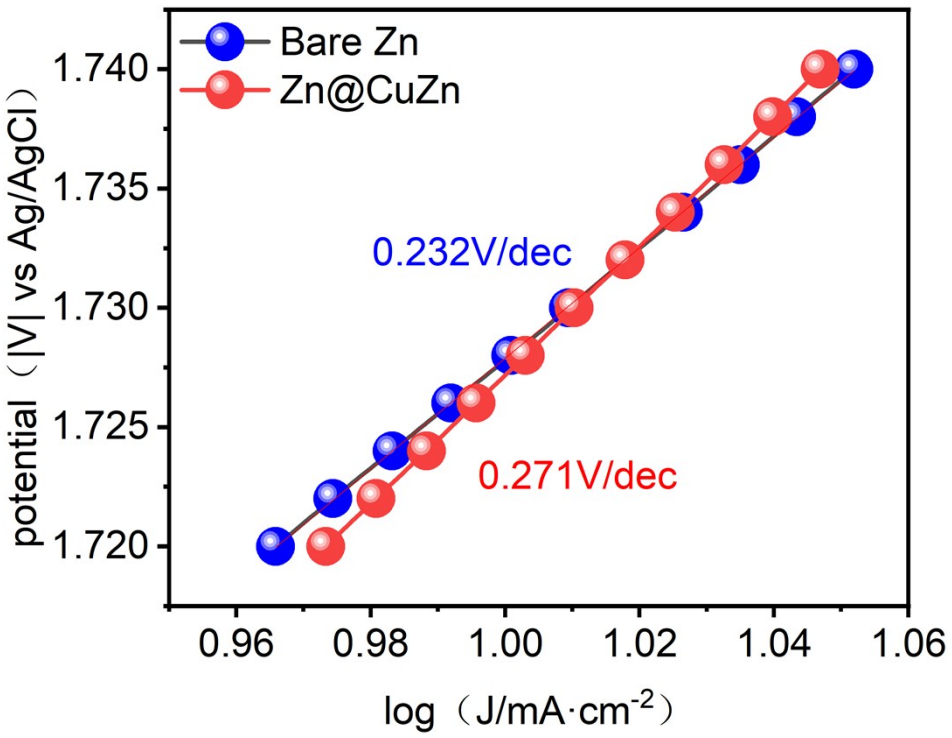

Figure S8. The HER Tafel curves of the bare Zn and Zn@CuZn.

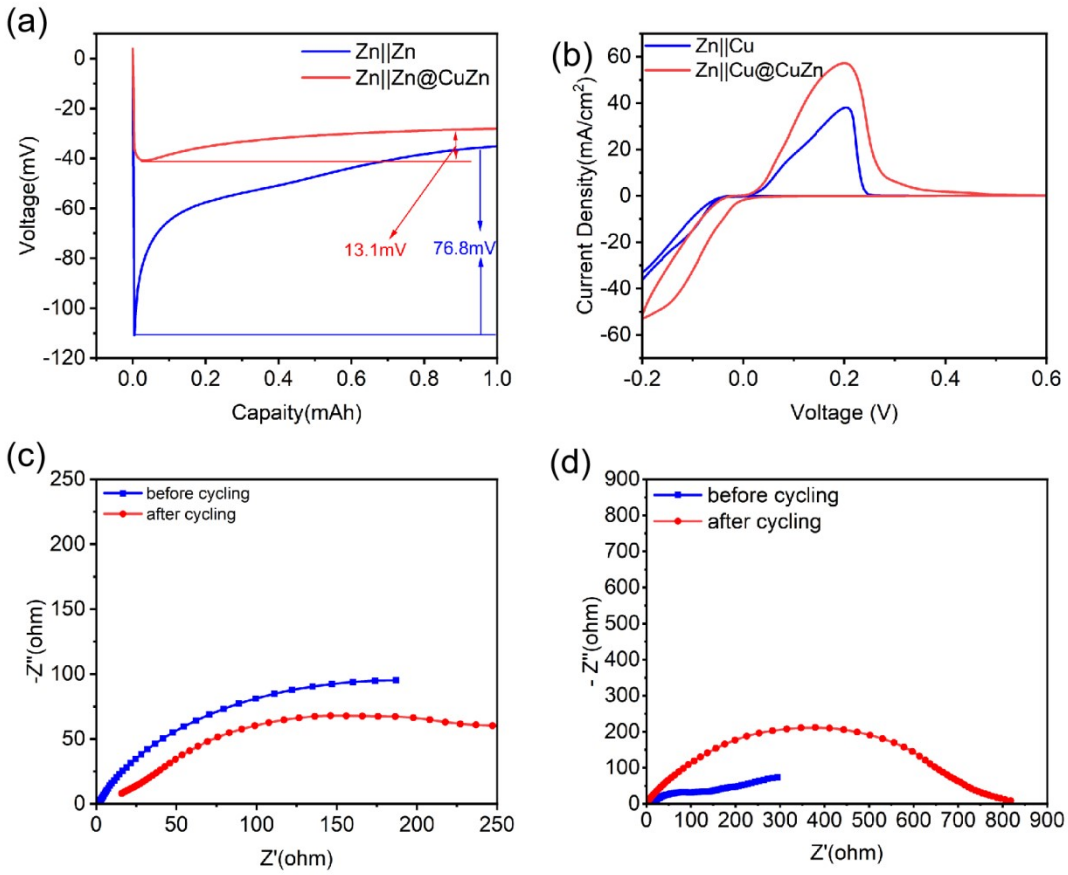

Figure S9. (a) Voltage capacity curves of Zn||Cu cell and Zn||Cu@CuZn at the current density of 1 mA cm^{-2}. (b) CV curves of Zn||Cu and Zn||Cu@CuZn asymmetric cells. The Nyquist plots of (c) Zn@CuZn and (d) bare Zn before and after cycling of the symmetric cells.

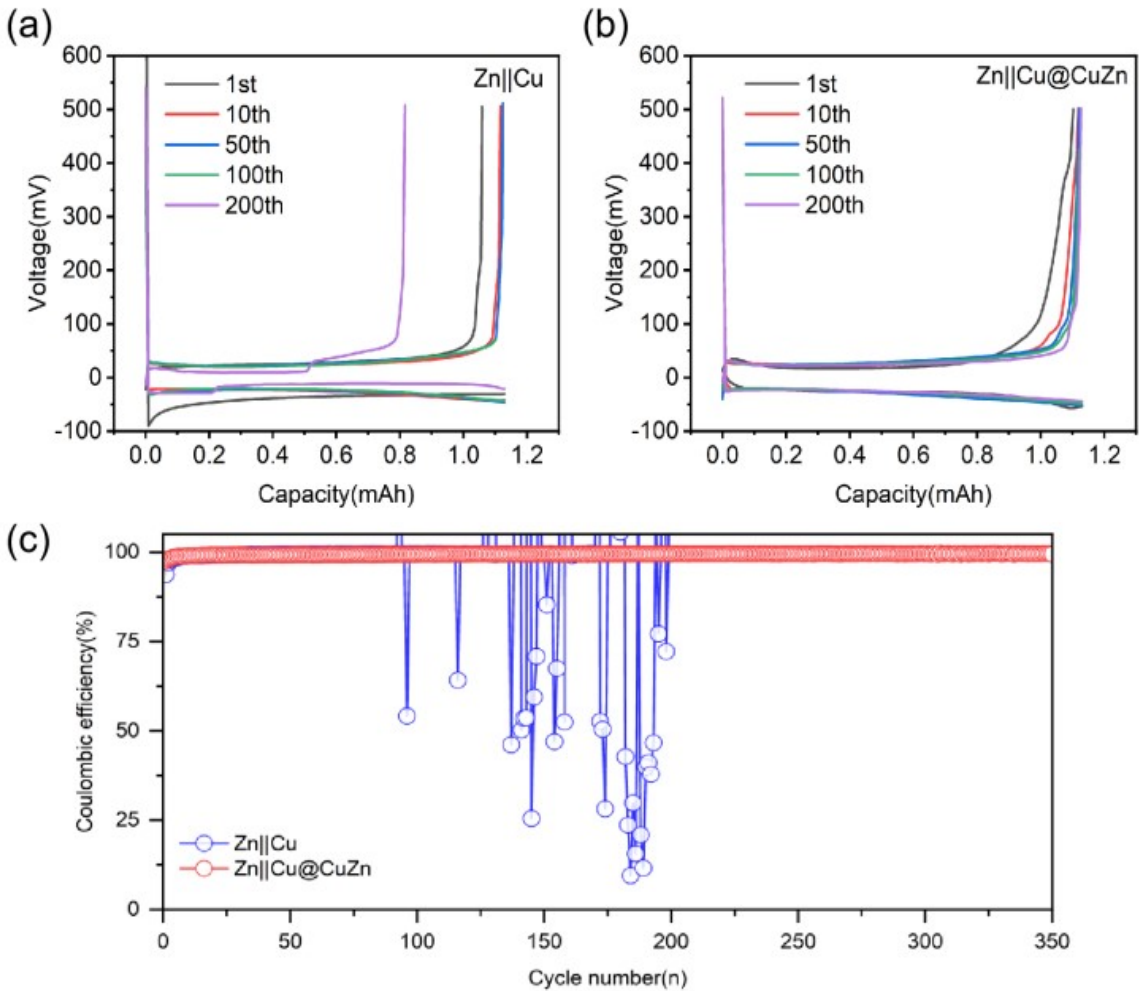

Figure S10. (a,b) The corresponding voltage profiles of Zn||Cu and Zn||Cu@CuZn asymmetric cells at 1 mA cm^{-2} with a plating capacity of 1 mAh cm^{-2}. (c) CEs of Zn||Cu and Zn||Cu@CuZn asymmetric cells at 1 mA cm^{-2} and 1 mAh cm^{-2}.

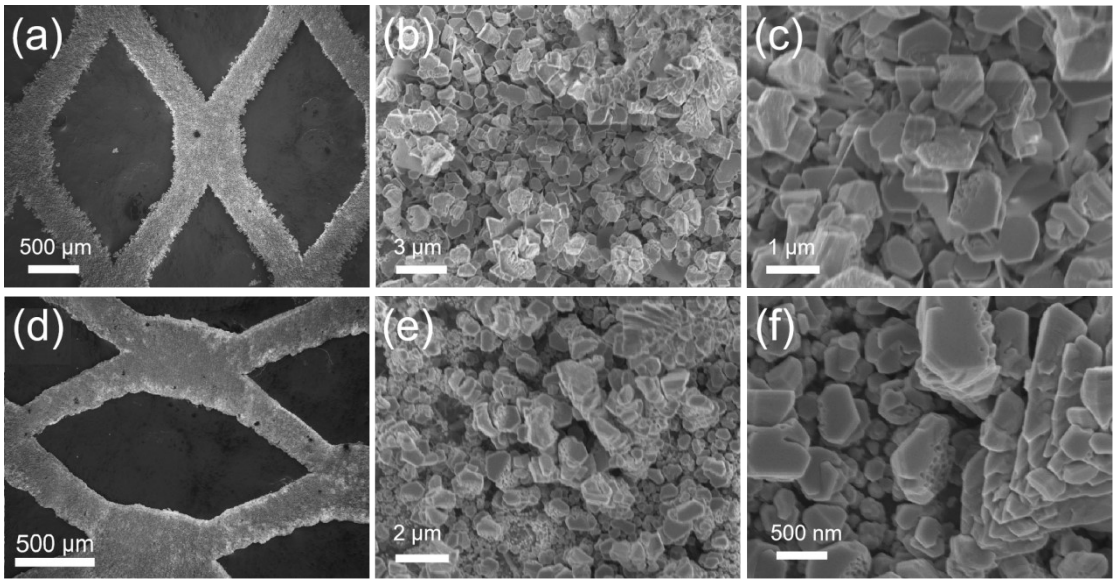

Figure S11. SEM images of (a-c) CuZn alloy coated Zn mesh1, (d-f) CuZn alloy coated Zn mesh2.

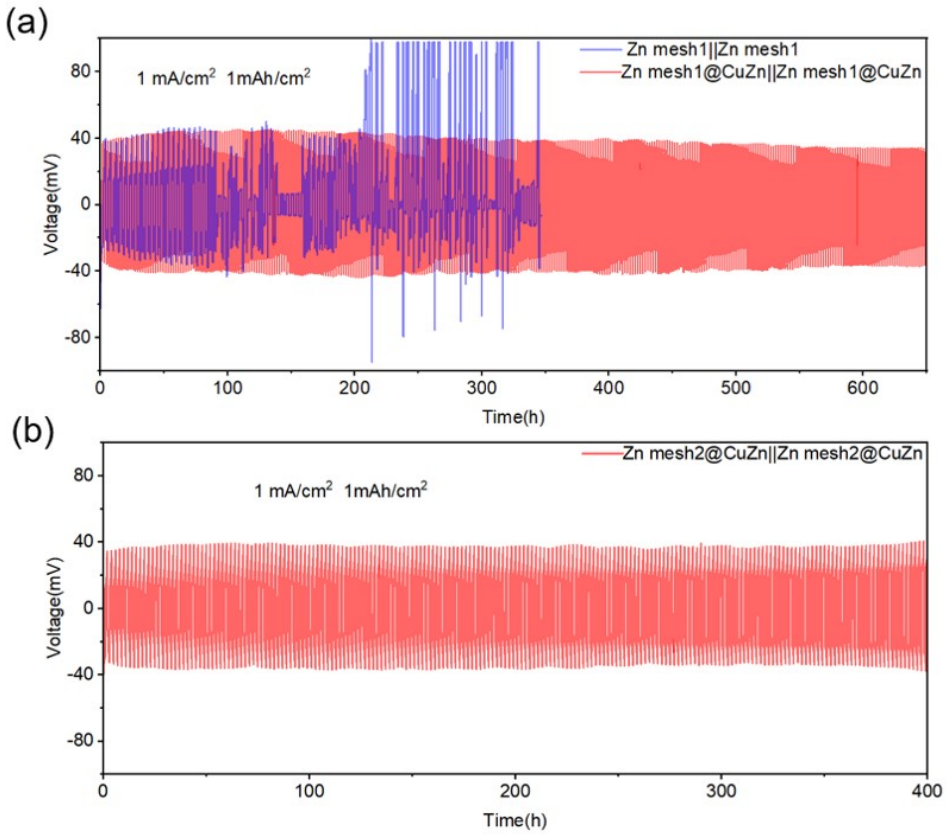

Figure S12. Cycling performance of (a) Zn mesh1||Zn mesh1 and Zn mesh1@CuZn||Zn mesh1@CuZn cells, (b) Zn mesh2@CuZn||Zn mesh2@CuZn cell at 1 mA cm^{-2} and 1 mAh cm^{-2}.

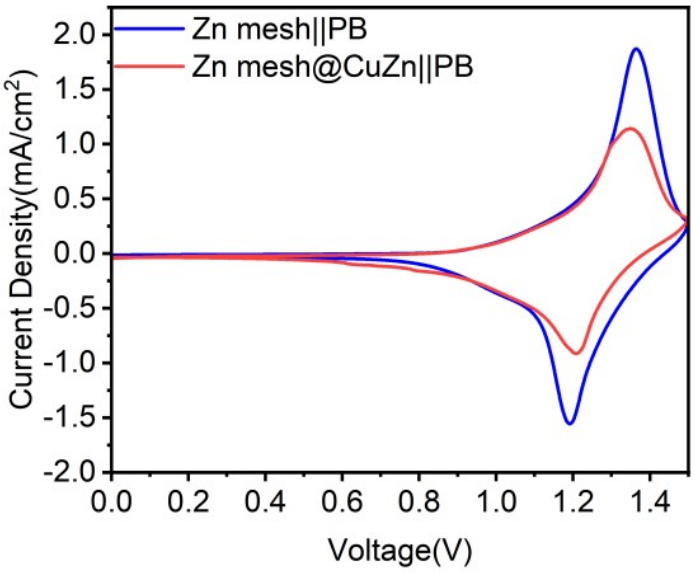

Figure S13. CV curves of Zn mesh||PB and Zn mesh@CuZn||PB.

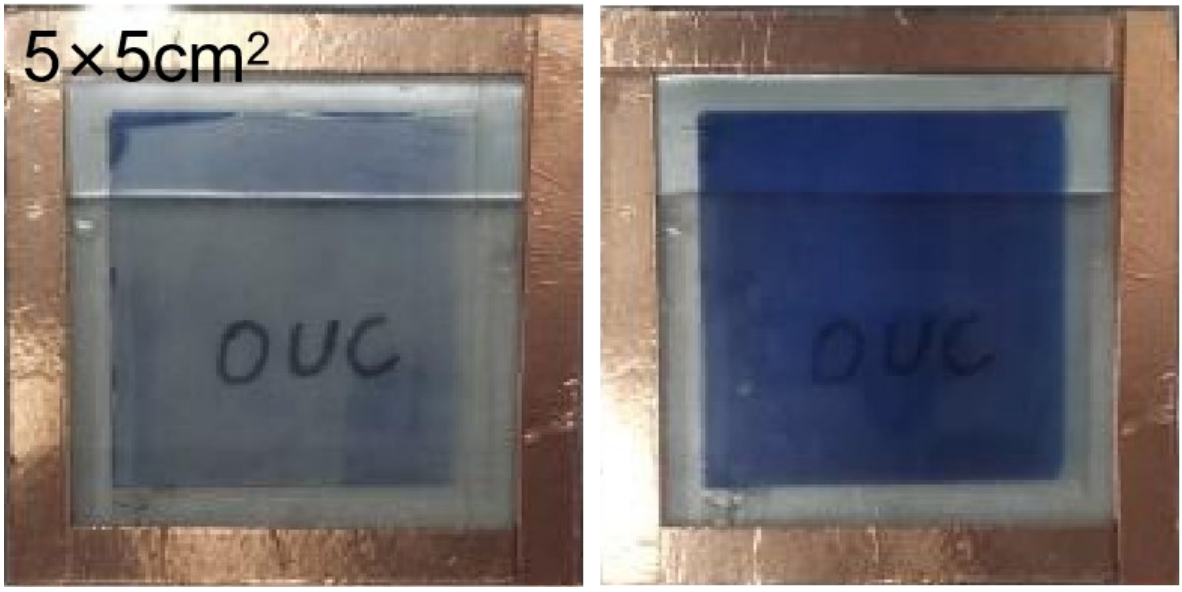

Figure S14. The optical photographs of the Zn mesh@CuZn||PB electrochromic device at bleached and colored states.

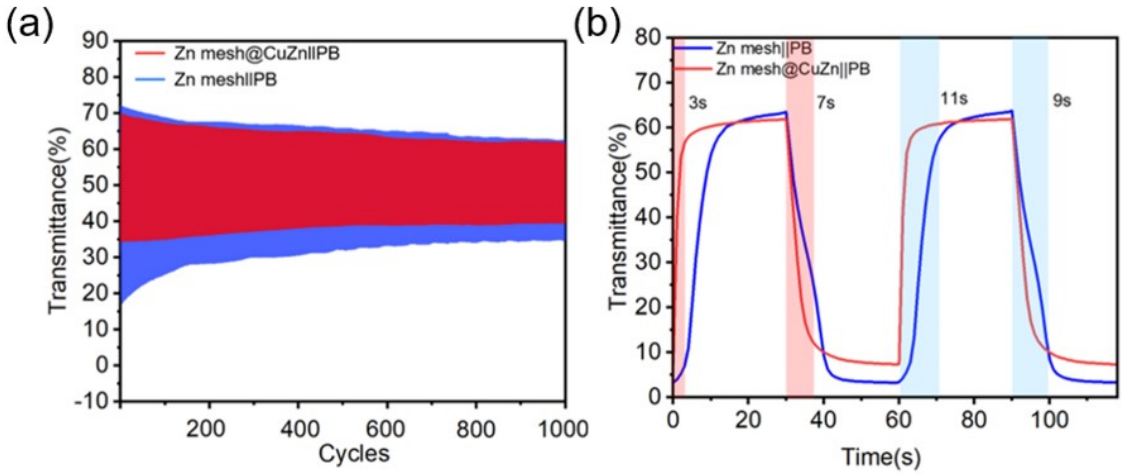

Figure S15. Dynamic transmittance modulation at 633 nm when switched between 1.5 V and 0 V for 30 s, respectively.

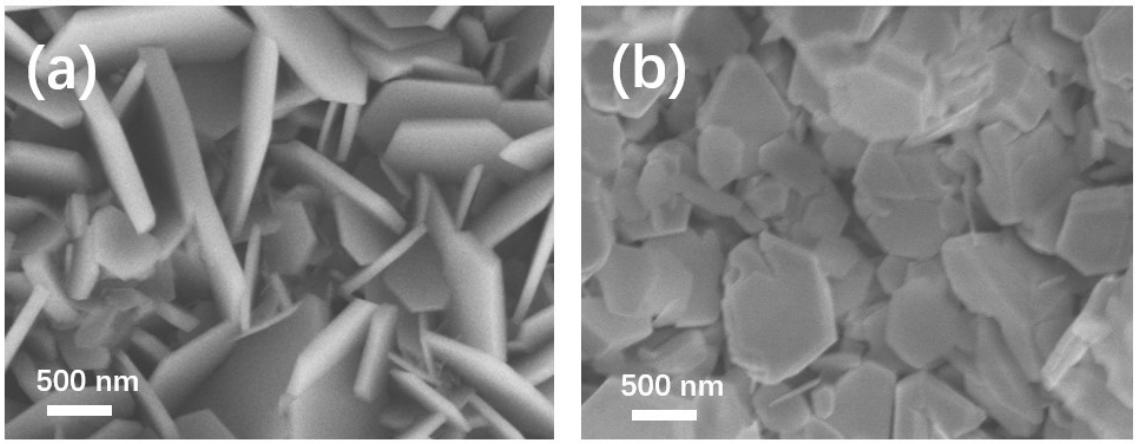

Figure S16. SEM images of (a) Zn mesh, and (b) Zn mesh@CuZn after 1000 cycles of the electrochromic devices.

Table S1. Zn anode performance comparison with reported studies.

	Overpotential（mV）	**Cycle time (h) of a modified symmetrical battery (x mA cm^{-2}, y mAh cm^{-2})**	**Modified zinc foil voltage hysteresis (mV) (x mA cm^{-2}, y mAh cm^{-2})**	**Average CE**
Zn@Ag[1]	23	350(1,1)	36(1,1)	
Zn@Au-NPs[2]	342	85(1,1)	90(1,1)	97.08% (60 cycles)
Zn@CCG[3]	41	160(0.9,0.9)	50(0.9,0.9)	99.3% (100 cycles)
ZnAl@Cu[4]		180(1,0.25)	67 (1,0.25)	99% (200 cycles)
Zn@Cu[5]	46	520(1,0.5)	30(1,0.5)	
This work	**13.1**	**600(1,1)**	**35(1,1)**	**99.4% (350 cycles)**

Reference

1. Lu, Q., Liu, C., Du, Y., Wang, X., Ding, L., Omar, A., Mikhailova, D. J. A. A. M., ACS Appl. Mater., 2021, **13** 16869.
2. Cui, M., Xiao, Y., Kang, L., Du, W., Gao, Y., Sun, X., Zhou, Y., Li, X., Li, H., Jiang, F., Zhi, C., ACS Appl. Energy Mater. 2019, **2**, 6490.
3. Bai, Y., Zhang, H., Tahir, M. U. Xiang, B. J. J. o. C., Colloid Interface Sci., 2022, **608**, 22.
4. Qi, Z., Xiong, T., Chen, T., Yu, C., Zhang, M., Yang, Y., Deng, Z., Xiao, H., Lee, W. S. V., Xue, J. J. A. A. M., ACS Appl. Mater. 2021, **13**, 28129.
5. Qian, Y., Meng, C., He, J., Dong, X. J. J. o. P. S., J. Power Sources 2020, **480**, 228871.